Search for electron decay mode e$\rightarrow\gamma + \nu$ with prototype of Borexino detector.

Abstract

The prototype of the Borexino detector Counting Test Facility, located in the Gran-Sasso laboratory, has been used to obtain a bound on the stability of the electron. The new lower limit on the mean lifetime defined on 32.1 days of data set is $\tau(e^- \rightarrow \nu_e + \gamma) \geq 4.6 \times 10^{26}$yr (90% c.l.).

H.O.Back[q], M.Balata[g], A. de Bari[i], T. Beau[c], A. de Bellefon[c], G.Bellini[a], J.Benziger[p], S.Bonetti[a], C.Buck[d], B.Caccianiga[a], L.Cadonati[p], F.Calaprice[p], G.Cecchet[i], M.Chen[b], A. Di Credico[g], O.Dadoun[c], D.D'Angelo[h], A.Derbin[l,t], M.Deutsch[o], F.Elisei[j], A.Etenko[m], F. von Feilitzsch[e], R.Fernholz[p], R.Ford[p], D.Franco[a], B.Freudiger[d], C.Galbiati[p], F.Gatti[h], S.Gazzana[g], M.G.Giammarchi[a], D.Giugni[a], M.Goeger-Neff[e], A.Golubchikov[a], A.Goretti[g], C.Grieb[e], C.Hagner[q], T.Hagner[e], W.Hampel[d], B.Harding[p], F.X.Hartmann[d], G.Heusser[d], A.Ianni[p,u], A.M.Ianni[p], H. de Kerret[c], J.Kiko[d], T.Kirsten[d], G.Korga[a,s], G.Korschinek[e], Y.Kozlov[m], D.Kryn[c], M.Laubenstein[g], C.Lendvai[e], P.Lombardi[a], I.Machulin[m], S.Malvezzi[a], J.Maneira[a], I.Manno[f], G.Manuzio[h], F.Masetti[j], A.Martemianov[g,r], U.Mazzucato[j], K.McCarty[p], E.Meroni[a], L.Miramonti[a], M.E.Monzani[a,g], P.Musico[h], H.Neder[d], L. Niedermeier[e], L.Oberauer*, M. Obolensky[c], F.Ortica[j], M.Pallavicini[h], L.Papp[a,s], L.Perasso[a], A.Pocar[p], R.S.Raghavan[n], G.Ranucci[a], W.Rau[g,d], A.Razeto[h], E.Resconi[h], A.Sabelnikov[a], C.Salvo[h], R.Scardaoni[a], S.Schoenert[d], H.Seidel[e], H.Simgen[d], T.Shutt[p], M.Skorokhvatov[m], O.Smirnov[l], A.Sonnenschein[p], A.Sotnikov[l], S.Sukhotin[m], V.Tarasenkov[m], R.Tartaglia[g], G.Testera[h], D.Vignaud[c], S.Vitale[h], R.B.Vogelaar[q], V.Vyrodov[m], M.Wojcik[k], O.Zaimidoroga[l], G.Zuzel[k].

a)Dipartimento di Fisica Universita' di Milano, Via Celoria, 16 I-20133 Milano, Italy;

b)Dept. of Physics, Queen's University Stirling Hall, Kingston, Ontario K7L 3N6, Canada;

c)Laboratoire de Physique Corpusculaire et Cosmologie, 11 place Marcelin Berthelot 75231 Paris Cedex 05, France;

d)Max-Planck-Institut fuer Kernphysik, Postfach 103 980 D-69029 Heidelberg, Germany;

e)Technische Universitaet Muenchen, James Franck Strasse, E15 D-85747 Garching, Germany;

f)KFKI-RMKI, Konkoly Thege ut 29-33 H-1121 Budapest, Hungary;

g)L.N.G.S. SS 17 bis Km 18+910, I-67010 Assergi(AQ), Italy;

h)Dipartimento di Fisica Universita' and I.N.F.N. Genova, Via Dodecaneso, 33 I-16146 Genova, Italy;

i)Dipartimento di Fisica Nucleare e Teorica Universita' di Pavia, Via A. Bassi, 6 I-27100, Pavia, Italy;

j)Dipartimento di Chimica Universita' di Perugia, Via Elce di Sotto, 8 I-06123, Perugia, Italy;

k)Institute of Physics, Jagellonian University, Cracow. ul. Reymonta 4. PL-30059 Krakow, Poland;

l)J.I.N.R. Joliot Curie str. 6, 141980, Dubna Moscow region, Russia;

m)RRC Kurchatov Institute, Kurchatov Sq.1, 123182 Moscow, Russia;

n)Bell Laboratories, Lucent Technologies, Murray Hill, NJ 07974-2070, U.S.A;

o)Department of Physics Massachusetts Institute of Technology, Cambridge, MA 02139, U.S.A.;

p)Department of Physics, Princeton University, Jadwin Hall, Washington Rd, Princeton NJ 08544-0708, USA;

q)Virginia Polytechnique Institute and State Univercity Blacksburg, VA 24061-0435, Virginia, U.S.A.;

r)on leave of absence from m;

s)on leave of absence from f;

t)on leave of absence from St. Petersburg Nuclear Physics Inst. - Gatchina, Russia;

u)presently at a;

$*$) Project manager.

1 Introduction

The U(1) gauge invariance of the QED Lagrangian dictates strict conservation of the electric charge and absence of the mass of the photon. The search for a violation of charge conservation (CC) is one of the possible tests when looking for physics beyond the Standard Model. The non-conservation of the electric charge (CNC) can be introduced in the Lagrangian by including additional interactions of leptons with photons in the form $g(\overline{e}\gamma_\alpha\nu + \overline{\nu}\gamma_\alpha e)A_\alpha$ or with Z-bosons in the form $G(\overline{\nu}\nu)(\overline{\nu}e)$. These interactions lead to the decay of the electron $e \to \gamma\nu$ or $e \to \nu\nu\nu$. An additional possibility is connected with CNC involving interactions with nucleons. Discussions of CNC in the context of gauge theories can be found in [1-10]. In these works one can find also the theoretical considerations showing that the decay $e \to \gamma\nu$ has to be accompanied by emission of a huge number of low energy photons against only one 255.5 keV photon[1], that we are looking for in the present paper.

The experimental limits on CC have been used recently to put very stringent limits on the Einstein equivalence principle [11].

Experimental tests of CC by searches for the decay mode with an emission of the photon or in invisible mode with neutrinos in the final state have a long experimental history [10],[12]-[24]. For the decay mode $e \to \gamma\nu$ the more stringent life time limit (2.0×10^{26} yr at 90% c.l.) was obtained with a 6.5 kg liquid xenon scintillator by the DAMA Collaboration with their detector devoted to the dark matter search [24]. The same collaboration with a 100 kg NaI(Tl) set-up set also the best limit for electron disappearance mode $e \to \nu\nu\nu$ from the atomic shell (2.4×10^{24} yr at 90% c.l.)[23]. CNC processes involving the hadronic sector in nuclei were studied in some experiments [25]-[29] and the more stringent limit was obtained from results of ^{71}Ga solar neutrino experiments $\Gamma(n \to p + 2\nu_e)$ / $\Gamma(n \to p + e + \nu_e) \leq 8 \times 10^{-27}$ at 68% c.l.[29]. For CNC processes that lead to the excitation of the atomic nuclei [30]-[33] the modern limits are $\varepsilon^2_W < 2.2 \times 10^{-26}$ and $\varepsilon^2_\gamma < 1.3 \times 10^{-42}$ at 90% c.l.[32], where ε^2_W and ε^2_γ give the relative strength of the CNC process to the corresponding CC process [8].

In this paper we present the results of $\gamma-$rays search with an energy $\simeq m_e/2$ following the $e \to \gamma\nu$ decay, using the prototype of the Borexino detector CTF (Counting Test Facility)[34]. The previous result was reported in [35].

2 Background measurements with prototype of Borexino (CTF).

Borexino, a real-time detector for low energy neutrino spectroscopy, is near completion in the underground laboratory at Gran Sasso (see recent [36] and references therein). The main goal of the detector is the direct measurement of the flux of ^7Be solar neutrinos of all

[1] the so called paradox of the unstable electron [1]. But in the modern view decaying electron is a paradox too. Detailed discussion one can find in [10] and references therein

flavours via neutrino-electron scattering in an ultra-pure liquid scintillator. Borexino will also address several other frontier questions in particle physics, astrophysics and geophysics.

The CTF was constructed and installed in Hall C of the Gran Sasso Laboratory. The main goal of the CTF was to test the key concept of Borexino, namely the possibility to purify a large mass of liquid scintillator at the level of contamination in U and Th of a few units 10^{-16} g/g. This goal was successfully achieved with the first prototype (CTF-I,[34]) operated in 1995-1997. The detector was reinstalled in 1999 (CTF-II,[37]) with the purpose of serving as a facility for the quality control of the pseudocumene to be delivered for the Borexino experiment. Although the CTF is a large-scale detector (4 tons of liquid scintillator), its size is nonetheless modest in comparison to Borexino (300 tons). The view of the CTF detector is presented in fig.1. A mass in the 4 ton range was set by the need to make the prevailing scintillator radioimpurities measurable via delayed coincidence tagged events[2], while a water shield thickness of approximately 4.5 m was needed in order to suppress the external radiation. The primary goal of the CTF was to develop a solution directly applicable to operational issues for Borexino; in the future there will be also the long-range goal of performing quality control during Borexino operations. Detailed reports on the CTF have been published [34],[36]-[40]. As a simplified scaled version of the Borexino detector, a volume of liquid scintillator is contained in a 2 m diameter transparent inner nylon vessel mounted at the center of an open structure that supports 100 phototubes (PMT) [41] which detect the scintillation signals. The whole system is placed within a cylindrical tank (11m in diameter and 10m height) that contains 1000 tons ultra-pure water, which provides a shielding against neutrons originating from the rock and against external γ-rays from PMT's and other construction materials. The scintillator used for the major part of tests in the CTF-I was a binary mixture consisting of pseudocumene[3] (PC) as a solvent and 1.5 g/l of PPO (2,5-diphenyloxazole) as a fluor. The CTF-II data analyzed in the present paper are acquired with an alternate liquid scintillator solvent, phenylxylylethane (PXE, $C_{16}H_{18}$)[4]. The scintillator is carefully purified to ensure the ^{238}U and ^{232}Th in it are less than some units 10^{-16} g/g. The PMT's are 8 inch ETL 9351 tubes made of low radioactivity glass and characterized by high quantum efficiency (26% at 420 nm), limited transit time spread (1 ns) and good pulse height resolution for single photoelectron pulses (Peak/Valley = 2.5). The number of photoelectrons registered by one PMT for the 1 MeV energy deposit at the detector's center is about 3.5 for the PXE.

[2]Key components in the decay chains of U/Th and in the β-decay of ^{85}Kr are emitted as time-correlated coincidence pairs which can be tagged with high specificity.

[3]1,2,4-trimethylbenzene C_9H_{12}

[4]with p-diphenylbenzene (para-terphenyl) as a primary wavelength shifter at a concentration of 3 g/l along with a secondary wavelength shifter 1,4-bis (2-methylstyrol) benzene (bis-MSB) at the 50 mg/l

3 Data processing and results

3.1 ^{14}C spectrum

The major part of the CTF background in the energy region up to 200 keV is induced by β-activity of ^{14}C. The β-decay of ^{14}C is an allowed ground-state to ground-state ($0^+ \rightarrow 1^+$) Gamow-Teller transition with an endpoint energy of $E_0 = 156$ keV and half life of 5730 yr. The beta energy spectrum with a massless neutrino can be written in the form [42]:

$$dN(E) \sim F(Z,E)C(E)pE(Q-E)^2dE \tag{1}$$

where

E and p are the total electron energy and momentum;

$F(E,Z)$ is the Fermi function with correction of screening by atomic electrons;

$C(E)$ contains departures from allowed shape.

For $F(E,Z)$ we used the function from [43] which agrees with tabulated values of the relativistic calculation [44]. A screening correction has been made using Rose's method [45] with screening potential $V_0 = 495$ eV. Although the β-decay of ^{14}C was investigated by many groups over almost 50 years, the situation with the shape factor is still unclear up to now [46]. The ^{14}C spectrum shape factor can be parametrized as $C(E) = 1 + \alpha E$. In the experiments [46],[47] the parameter α was measured to be $\alpha \simeq -1.0 \pm 0.04\ MeV^{-1}$ in good agreement with theoretical predictions of [48]. But in experiment [49] a value $\alpha \simeq -0.45 \pm 0.04\ MeV^{-1}$ was obtained, which is consistent with other theoretical calculations [50],[51].

In our calculation we leave this parameter free in order to avoid errors caused by the parameter uncertainty.The values parameter α takes during the minimization of the likelihood function are in the interval $-0.8 < \alpha < -0.72$, which are not ruled out nor by the theory nor by the experiments.

3.2 Ionization quenching

The light yield for the electrons can be considered linear with respect to its energy only for the high energies. At the lower energies the phenomenon of the "ionization quenching" violates the linear dependence of the light yield on energy. The explanation of this phenomenon has been presented by Birks in [52]. The Birks model subdivides the excited molecules into two classes, damaged and undamaged. The presence of the damaged molecules quenches the scintillation because they drain energy which would otherwise be released through luminescence. Following the model [52], the scintillation yield Y can be expressed in differential way by the relation

$$\frac{dY}{dx} \sim \frac{\frac{dE}{dx}}{1 + kB\frac{dE}{dx}}, \tag{2}$$

where the ratio between the "damaged" and "undamaged" molecula is $B\frac{dE}{dx}$ and the quenching probability is k. The product of these two parameters is usually treated as a

single parameter k_B. The light yield suppression for the $k_B = 0.015$ cm/MeV calculated numerically in [53] is shown in the fig.2 by points with error bars.

The effect on the electrons and gammas light yield is discussed in [53]. The factor $k_B = 0.0167 \pm 0.0015$ cm/MeV has been measured for the scintillator on the base of pseudocumene [54]. The present data are taken with detector loaded with scintillator on the base of PXE. No direct measurements of the quenching for this scintillator are available. Nevertheless, the comparison of the available data can provide reasonable estimation of the parameter. In [53] are presented the data for eight scintillating mixtures, the k_B values ranges from 0.0091 to 0.0149 cm/MeV. The scintillators having higher light yield demonstrate higher k_B values. As the light yield of the scintillator on the base of PC (3.6 p.e./PMT for the 1 MeV event at the detector's center) is slightly higher than the light yield of the scintillator on the base of PXE (3.5 p.e./MeV/PMT), the choice of the smaller value of k_B is appropriate. In our estimations we used $k_B = 0.015$ cm/MeV. It should be noted that choice of other k_B values in not influencing the result. The choice of any k_B in the range from 0.01 up to 0.02 changes our result by no more than 4%.

Noting that the function in fig.2 has $1 - e^{-x}$ behaviour, we used for the calculation the parameterization of the light yield dependence on energy $f(k_B, E)$ with three fixed parameters in the following form:

$$f(k_B, E) \equiv \frac{Y(E)}{Y(\infty)} = C_1 exp(-\frac{E^{C_2}}{C_3}). \tag{3}$$

The parameters were defined fitting the data with $1 - f(k_B, E)$ function. The light yield deficit function $\frac{\Delta Y}{Y(\infty)} = \frac{Y(E)-Y(\infty)}{Y(\infty)} \equiv 1 - f(k_B, E)$ is shown in the fig.2 by the solid line.

The presence of the strong ^{40}K peak in the CTF-II data gives the possibility to check the correctness of our k_B choice (see 3.5).

3.3 Detector resolution

The detailed analysis of the CTF energy resolution can be found in [55]. Because of the nonlinear dependence of the light yield on the energy released due to the ionization quenching effect, the CTF resolution should be expressed in the terms of the total registered charge, which is directly measured in the experiment. Taking into account the dependence of the registered charge on energy one can write for the CTF relative charge resolution:

$$\frac{\sigma_Q}{Q} = \sqrt{\frac{1 + \overline{v_1}}{A \cdot E \cdot f(k_B, E) \cdot v_f} + v_p}, \tag{4}$$

where

$\overline{v_1} = \frac{1}{N_{PM}} \sum_{i=1}^{N_{PM}} s_i v_{1_i}$ is the relative variance of the PMT single photoelectron charge spectrum (v_{1_i}) averaged over all CTF PMTs (N_{PM}), taking into account the i-th PMT relative sensitivity s_i;

A is scintillator light yield measured in photoelectrons per MeV ($A \equiv \frac{Y(\infty)}{E}$, A=350 p.e./MeV in CTF);

$f(k_B, E)$ is the function taking into account ionization quenching, the function is defined by (3);

v_p is the parameter which takes into account the variance of the signal for the source uniformly distributed over the detector's volume. Because of the detector's spherical symmetry one can describe the dependence of the registered charge on the distance from the event to the detector's center **r** with a function of **r**, $Q(r) = Q_0 f_R(r)$, where Q_0 is the charge collected for the event of the same energy occurred at the detector's center. The v_p parameter is the relative variance of the $f_R(r)$ function over the detector volume:

$$v_p \equiv \frac{< f_R^2(r) >_V}{< f_R(r) >_V^2} - 1;$$

v_f is volume factor, coming from the averaging of the signals over the CTF volume, $v_f \equiv \frac{<Q(r)>_V}{Q_0}$.

For the details of the parameters meaning see [55].

All the parameters (with exception of the light yield A) in (4) can be defined independently with satisfactory precision. The PMT charge spectra have been studied during the PMT acceptance tests, the relative charge spectrum variance is known for each PMT in the detector. The relative sensitivities can be easily extracted from the data, comparing the mean values of the PMT charge spectra for a well defined source (for example ^{214}Bi–^{214}Po events that can be tagged with a delayed coincidence). The evaluation of the parameter $\overline{v_1}$ gives the value of 0.34 with a precision of about 5%. Since this value is summed with 1, one can fix the value without introducing further error.

The v_p and v_f were estimated from the correlated ^{214}Bi–^{214}Po (radon) data. The total number of radon events is 1358 during 32.1 days. In the analysis we assumed that all these events are uniformly distributed over the CTF inner vessel. First all the ^{214}Bi–^{214}Po events were considered and the charge resolution for the ^{214}Po was estimated. Then the events of the ^{214}Bi–^{214}Po chain occurring in the central region (r=50 cm of the total 100 cm) were considered. The comparison of the resolution for these two cases gives the value $v_p = 0.0023$, and the comparison of the mean values gives $v_f = 1.005$. These values were fixed for the calculations.

The radial dependence of the detector response (total collected charge) was defined using the radon data as well.

For the estimations of the energy resolution one can use approximation $\frac{\sigma_E}{E} \approx \frac{\sigma_Q}{Q}$. The full absorption peak of the 256 keV gamma corresponds to 210 keV on the scale calibrated with electrons, the resolution at this energy is $\sigma_E \approx 30.4$ keV (or 72 keV FWHM resolution) for $A = 350$ and $v_1 = 0.34$. The resolution is rather poor in comparison to the germanium detectors, while the inner electron binding energy is about 40 times less, this allows us to neglect the Doppler broadening of the 256 keV gamma line (see [10, 17, 20, 21]). The maximum effect of the Doppler broadening will lead to the superimposed gaussian with

$\sigma_C(K) = 6.3$ keV (for the case of the carbon K-electron with 283 eV binding energy), which will give neglegible contribution of about 2% to the overall detector's resolution.

3.4 Data selection and fitting function

In our analysis we used the data obtained with an upgrade of the CTF detector, CTF-II. The detector, loaded with the PXE, is equipped with an additional nylon bag (radon shroud) intended to reduce the radon diffusion from the construction materials into the scintillator.

The data obtained during 32.1 days of the CTF-II run were used. The data are contaminated with the soft part of the spectra of beta and γ coming from the decay of ^{40}K[5]. A specific analysis has been performed, showing that the source is outside the inner vessel [37],[56]. In fig.3 the radial distribution of the events in two different energy intervals are plotted. One can see that the proper spatial cut can eliminate part of the ^{40}K events, leaving major part of the ^{14}C events. The study of the optimal cut have been performed, with a cut radius varying from R=90 cm to R=110 cm, the final goal was to provide maximal surface background reduction with a minimal losses of the uniformly distributed over the detector's volume ^{14}C events. It was found that optimal ratio between the background reduction and detector's effective volume is achieved at R=100 cm. Using this cut the background reduction of the factor 5 in the energy region about 200 keV was achieved. At the same time only about 30% of the ^{14}C spectrum is lost in the region of interest. It should be noticed, that ^{40}K events at the lower energies are reconstructed mainly outside of the inner vessel. This is caused by the difference of the refraction indexes of the scintillator and water which is not properly accounted for in the reconstruction program. We used the reconstructed radius only as a parameter of the spatial cut in our analysis, the effective volume decrease was estimated independently by the decrease of the ^{14}C count. In such a way no error is introduced because of the misplaced events.

Another possibility to reduce the background is to remove signals identified as muons by the muon veto system. The pulse shape analysis provides the possibility to distinguish between the signals caused by electrons and alpha- particles. In fig.4 all these cuts are shown.

The residual spectrum in addition to the ^{14}C has the contribution of the other sources. This background is practically linear in the region 220-450 keV, and one can expect the same linear behaviour down to the lower limit used (138 keV). Monte Carlo simulations were performed to confirm the linear behaviour of this contribution the the total background. The simulation based on the measurements performed for the CTF-I detector indicate that the shape of the background underlying the ^{14}C $\beta-$spectrum has a small, constant slope for energies between 60 and 500 keV [38].

[5] ^{40}K has two decay channels:
$^{40}K \rightarrow ^{40}Ca\,(\beta)$, 89.3%, $Q = 1.311\,MeV$,
$^{40}K \rightarrow ^{40}Ar\,(EC)$, 10.7%, $Q = 1.505\,MeV$,
the latter one is followed by the emission of 1.46 MeV γ.

The part of the spectrum starting at 138 keV has been used in the analysis in order to avoid the spectrum distortions introduced by the threshold effect. The choice of the lower limit is defined by the resolution of the detector and quite high threshold. The threshold itself is not defined well in the terms of energy. In the CTF-II the trigger has been adjusted to 21 fired electronics channels. The CTF-II electronics consists of 64 channels connected to 100 PMTs. In such a way, major part of the PMTs are coupled to single electronics channel. The effect of the trigger can be illustrated by the following. The mean number of channels fired for the event with an energy E at the detector's center is:

$$< N >= N_S(1 - e^{-\mu_0}) + N_F(1 - e^{-2\mu_0}), \tag{5}$$

where μ_0 is the mean number of photoelectrons registered by one PMT in the event, $N_S = 28$ is the number of the single channels and $N_F = 36$ is the number of the channels connected to two PMTs. The solution of (5) for <N>=21 will yield $\mu_0 = 0.26$, i.e. a total collected charge of 26 p.e. This value is the detector threshold in the sense that only 50% of the events with an energy corresponding to this charge are registered. Of course, this causes a significant spectrum deformation near the threshold. In order to avoid these deformations one should set the threshold at the level that will cut the events with energies that are not providing practically 100% registration, within 3σ interval it will give $Q_{th} + 3\sigma_{Q_{th}} = 26 + 3.\sqrt{1.34 \cdot 26} = 43.7$ p.e. This charge corresponds to the energy release of 135 keV at the detector's center.

The lower limit was estimated with Monte Carlo method taking into account the spatial distribution of the events, the electronics threshold (the electronics channel is fired if signal on the input overcomes discriminator threshold set at 0.2 p.e. level) and the map of working PMTs. The simulation gives 45 p.e. lower limit (or 138 keV) which is very close to the one obtained with the simple estimation using (5).

3.5 Response function for the 256 keV γ

The Monte- Carlo method has been used in order to simulate the CTF response to the 256 keV gamma. The hypothetical electron decay can occur in the scintillator as well as in water. The decays in scintillator and in water were simulated separately and then summed taking into account the number of the candidate electrons. The response function was normalized to one electron decay in the scintillator volume.

The program generates random positions inside the inner vessel (or in the water layer of 30 cm) and follows the gamma- electron shower using the EGS-4 code[57]. As soon as an electron of energy E_e is to appear inside the in scintillator, the corresponding charge is added to the running sum:

$$\Delta Q = E_e \cdot f(k_B, E_e) \cdot A \cdot f_R(r), \tag{6}$$

where $f_R(r)$ is a factor, taking into account the dependence of the registered charge on the distance from the detector's center. On the next step a random charge is generated in accordance to the normal distribution with a mean value of $Q = \sum \Delta Q$ and with variance

σ_Q defined by formula (4). Finally, the radial reconstruction error was simulated in order to take into account the spatial cut applied.

The presence of the strong gamma line of 1.46 MeV in the CTF-II data provides a possibility to check the model used. The gamma with 1.46 MeV energy comes from the decays of ^{40}K outside the inner vessel. The data together with the results of MC simulation are shown in the fig.5. One can see good agreement of the Monte-Carlo simulated position of the ^{40}K with the position of this full absorption peak in the data.

Another study was performed using ^{85}Kr data in the CTF-I detector. ^{85}Kr decays into an excited state of the ^{85}Rb (with a probability of 0.43%), producing a beta of maximum energy of 173 keV followed by emission of a 514 keV γ with 1.01 μs half-life time. These events being well identified by a delayed coincidence, present a very nice source for the calibration at 514 keV. The Monte Carlo simulated position appears in a good agreement with the data (peak about 440 keV)[53].

3.6 Analysis

As it was pointed out in section 3.4, the CTF-II spectrum has been studied in the 138-300 keV region.

All the analysis was performed on the charge scale (total collected charge summed over all PMTs), and only the final plots are converted to the energy scale.

The convolution of the ^{14}C beta spectrum with the detector's resolution (4) with an additional linear background have been used as a model function:

$$S(Q) = N_0 \int N(E(Q'))\frac{dE}{dQ} Res(Q, Q')dQ' + LinBkg(Q) \tag{7}$$

where $Res(Q, Q') = \frac{1}{\sqrt{2\pi}\sigma_Q} e^{-\frac{1}{2}(\frac{Q-Q'}{\sigma_Q})^2}$ is the detector response function, σ_Q is defined by (4);

N(E) is the ^{14}C beta- spectrum (1);

the total collected charge Q is defined by $Q(E) = A \cdot E \cdot f(k_B, E)$.

The parameters of the linear part of the spectrum were defined in the flat region of the total spectrum (250-400 keV) and fixed in the further analysis.

On the first step we leave light yield A to be a free parameter of the fit together with the total normalization and the ^{14}C shape factor α. Then the check on the ^{40}K data was performed (see 3.5 and fig.5). The good agreement between the data and Monte-Carlo simulations of ^{40}K gammas, together with the good quality of the raw data fit itself ($\chi^2 = 134.5/146$), allows us to fix light yield in the further analysis at the value obtained on this step, namely 3.56 p.e/PMT/MeV.

On the next stage of the analysis we add the admixture of the 256 keV gamma to the model function (7). The total normalization N_0 of the ^{14}C spectrum and the ^{14}C shape factor α were the only free parameters in the model. The likelihood function was found from the assumption that the number of counts in each channel obeys a normal distribution, and represents the sum of the model function (7) and the response function

to the 256 keV gamma found with the MC method. The analysis of the likelihood function gives us the value of $S \leq 170$ decays at the 90% c.l.

The limit on the lifetime was calculated by the formula

$$\tau \geq \varepsilon N_e \frac{T}{S}, \tag{8}$$

where

$N_e = 1.36 \times 10^{30}$ is a number of electrons inside scintillator ;

$T = 32.1$ days- time of measurement;

$S = 170$ is an upper limit on the number of counts of response function inside the fitting interval;

$\varepsilon = 0.67-$the part of the events survived after the spatial cut applied. The last number was estimated from the number of ^{14}C events lost in the region around 150 keV after the spatial cut.

The likelihood function for the S=0 reaches its maximum at $\alpha = -0.72$, and for the $S = 170$ at $\alpha = -0.8$.

4 Conclusion

The new lower limit on the mean lifetime for the decay e$\rightarrow\gamma+\nu$ has been established using the results of the liquid scintillator detector CTF-II, $\tau \geq 4.6 \times 10^{26}$yr (90% c.l.).

References

[1] L.B.Okun, Ya.B.Zeldovich, Phys.Lett. 78B (1978) 597

[2] M.B.Voloshin, L.B.Okun, JETP Lett., 28 (1978) 145

[3] A.Y.Ignatiev, V.A.Kuzmin, M.E.Shaposhnikov, Phys.Lett.84B (1979) 315

[4] A.D.Dolgov, Ya.B.Zeldovich, Rev.Mod.Phys.53 (1981) 1

[5] L.B.Okun, Leptons and Quarks (North Holland, Amsterdam) (1982) 181

[6] M.Suzuki, Phys.Rev., 38D (1988) 1544

[7] L.B.Okun, Comments Nucl.Part.Phys., 19 (1989) 99

[8] J.N.Bahcall, Neutrino Astrophysics (Cam. Un. Press, England) (1993) 360

[9] H.Ejiri, H.Kinoshita, H.Sano, H.Ohsumi, Phys.Lett. 282B (1992) 281

[10] Y.Aharanov, F.T.Avignone III, R.L.Brodzinski, J.I.Callar, E.Garsia, H.S.Miley, A.Morales, J.Morales, S.Nussinov, A. Ortiz de Solorzano, J.Puimedon, J.H.Reeves, C.Saenz, A.Salinas, M.S.Sarsa, J.A.Villar, Phys.Rev. 52D (1995) 3785

[11] S.Landau, P.D.Sisterna, H.Vucetich. gr-qc/0105025, 2001.

[12] G.Feinberg, M.Goldhaber, Proc.Nat.Acad.Sci. USA, 45 (1959) 1301

[13] M.K.Moe, F.Reines, Phys.Rev. 140 (1965) 992

[14] F.Reines, H.W.Sobel, Phys.Rev.Lett. 32 (1974) 954

[15] R.I.Steinberg, K.Kwiatowski, W.Maenhout, N.S.Wall Phys.Rev. 12D (1975) 2582

[16] E.L.Kovalchuk, A.A.Pomanski, A.A.Smolnikov, JETP Lett., 29 (1979) 145

[17] E.Bellotti, M.Corti, E.Fiorini, C.Liguori, A.Pullia, A.Saracino, P.Sverzellati, L.Zanotti, Phys.Lett. 124B (1983) 435

[18] F.T.Avignone III, R.L.Brodzinski, W.K.Hensley, H.S.Milley, J.H.Reeves, Phys.Rev. 34D (1986) 97

[19] D.Reusser, M.Treichel, F.Boem, C.Broggini, P.Fisher, L.Fluri, K.Gabathuler, H.Herikson, V.Jorgens, L.W.Mitchell, C.Nussbaum, J.LVuilleumier, Phys.Lett. 225B (1991) 143

[20] A.Balysh, M.Beck, S.Belyaev, F.Bensh, J.Bockholt, A.Demehin, A.Gurov, G.Heusser, H.V.Klapdor-Kleingrothous, I.Kondratenko, V.Lebedev, B.Maier, A.Muller, F.Petry, A.Piepke, H.Strecker, K.Zuber, Phys.Lett. 298B (1993) 278

[21] Y.Aharanov, F.T.Avignone III, R.L.Brodzinski, J.I.Callar, E.Garsia, H.S.Miley, A.Morales, J.Morales, S.Nussinov, A. Ortiz de Solorzano, J.Puimedon, J.H.Reeves, C.Saenz, A.Salinas, M.S.Sarsa, J.A.Villar, Phys.Lett. 353B (1995) 168

[22] P.Belli, R.Bernabei, W.Di Nicolantonio, V.Landoni, A.Incicchitti, D.Prosperi, C.J.Dai, C.Bacci, Astropart.Phys. 5 (1996) 217

[23] P.Belli, R.Bernabei, C.J.Dai, H.L.He, G.Ignesti, A.Incicchitti, H.H.Kuang, J.M.Ma, F.Montecchia, O.A.Ponkratenko, D.Prosperi, V.I.Tretyak, Yu.G.Zdesenko, Phys.Lett. 460B (1999) 236

[24] P.Belli, R.Bernabei, C.J.Dai, G.Ignesti, A.Incicchitti, F.Montecchia, O.A.Ponkratenko, D.Prosperi, V.I.Tretyak, Yu.G.Zdesenko, Phys.Rev. 61D (2000) 117301

[25] A.W.Sunyar, M.Goldhaber, Phys.Rev. 120 (1960) 871

[26] E.B.Norman, A.G.Seamster, Phys.Rev.Lett. 43 (1979) 1226

[27] I.R.Barabanov et al., JETP Lett. 32 (1980) 359

[28] A.Roy et al., Phys.Rev. D28 (1983) 1770

[29] E.B.Norman, J.N.Bahcall, M.Goldhaber Phys.Rev. D53 (1996) 4086

[30] S.Noljevic et al., Phys.Rev. C35 (1987) 341

[31] H.Ejiri, M.Kawasaki, H.Kinoshita et al., Phys. Rev. C44 (1991) 502

[32] P.Belli, R.Berbabei, C.J.Dai, G.Ignesti, A.Inciccitti, F.Montecchia, O.A.Ponkratenko, D.Prosperi, V.I.Tretyak, Yu.G.Zdesenko, Phys.Lett. 465B (1999) 315

[33] P.Belli, R.Bernabei, C.J.Dai et al., Phys.Rev. C60 (1999) 065501

[34] Borexino Collaboration, G.Alimonti et al., Nucl.Instr.Meth. A406 (1998) 411

[35] C.Galbiati, R.Dossi, S.Schoenert on behalf of the Borexino collaboration, XVII Physics in Collision, Poster Session, Villa Aldobrandini, Frascati, June 18th-19th, 1998

[36] Borexino Collaboration, G.Alimonti et al., Astrop.Journal 2001

[37] E. Resconi, "Measurements with the Upgraded Counting Test Facility (CTF-2) of the Solar Neutrino Experiment Borexino", Doctorate Thesis, Universita' degli Studi di Genova, 2001

[38] Borexino Collaboration, G.Alimonti et al., Phys.Lett. B422 (1998) 349

[39] Borexino Collaboration, G.Alimonti et al., Astroparticle Phys. 8 (1998) 141

[40] Borexino Collaboration, G.Alimonti et al., Nucl.Instr.Meth. A440 (2000) 360

[41] G.Ranucci et al., Nucl.Instr.Meth. A333 (1993) 553

[42] M.Morita, Beta Decay and Muon Capture, Benjamin, Reading, Mass., (1973) 33

[43] J.J.Simpson, A.Hime, Phys.Rev. 39D (1989) 1825

[44] H.Behrens, J.Janecke, Numerical Tables for beta-decay and electron capture, ed. H.Schopper, Landolt-Bornstein, Springer, Berlin, 4 (1969)

[45] M.E.Rose, Phys.Rev. 49 (1936) 727

[46] V.V.Kuzminov, N.Ia.Osetrova, Physics of Atomic Nuclei, 63 (2000) 1292

[47] B.Sur, E.B.Norman, K.T.Lesko et al., Phys.Rev.Lett. 66 (1991) 2444

[48] H.Genz, G.Kuhner, A.Richter, H.Behrens, Z.Phys. A341 (1991) 9

[49] F.E.Weifeld, E.B.Norman, Y.D.Chan et ai., Phys.Rev., C52 (1995) 1028

[50] F.P.Calaprice, B.R.Holstein, Nucl.Phys. 273A (1976) 301, 23.

[51] A.Garcia, B.A.Brown, Phys.Rev. 52C (1995) 34

[52] J.B.Birks, Proc.Phys.Soc. A64 (1951) 874.

[53] S.Bonetti, O.Donghi, C.Salvo, G.Testera. "Ionization quenching: effects on e^- and γ detection in Borexino and in CTF". Borexino internal report 98/10/15, 1998.

[54] M.N.Peron. Private communication.

[55] O.Smirnov. Resolutions of a large volume liquid scintillator detector. LNGS preprint INFN TC/00/17 (2000).

[56] L.Cadonati. Borexino internal report, 00/08/27 (2000).

[57] Walter R. Nelson, Hideo Hirayama, David W. O. Rogers. The EGS4 code system. SLAC-265, 1985.

List of Figures

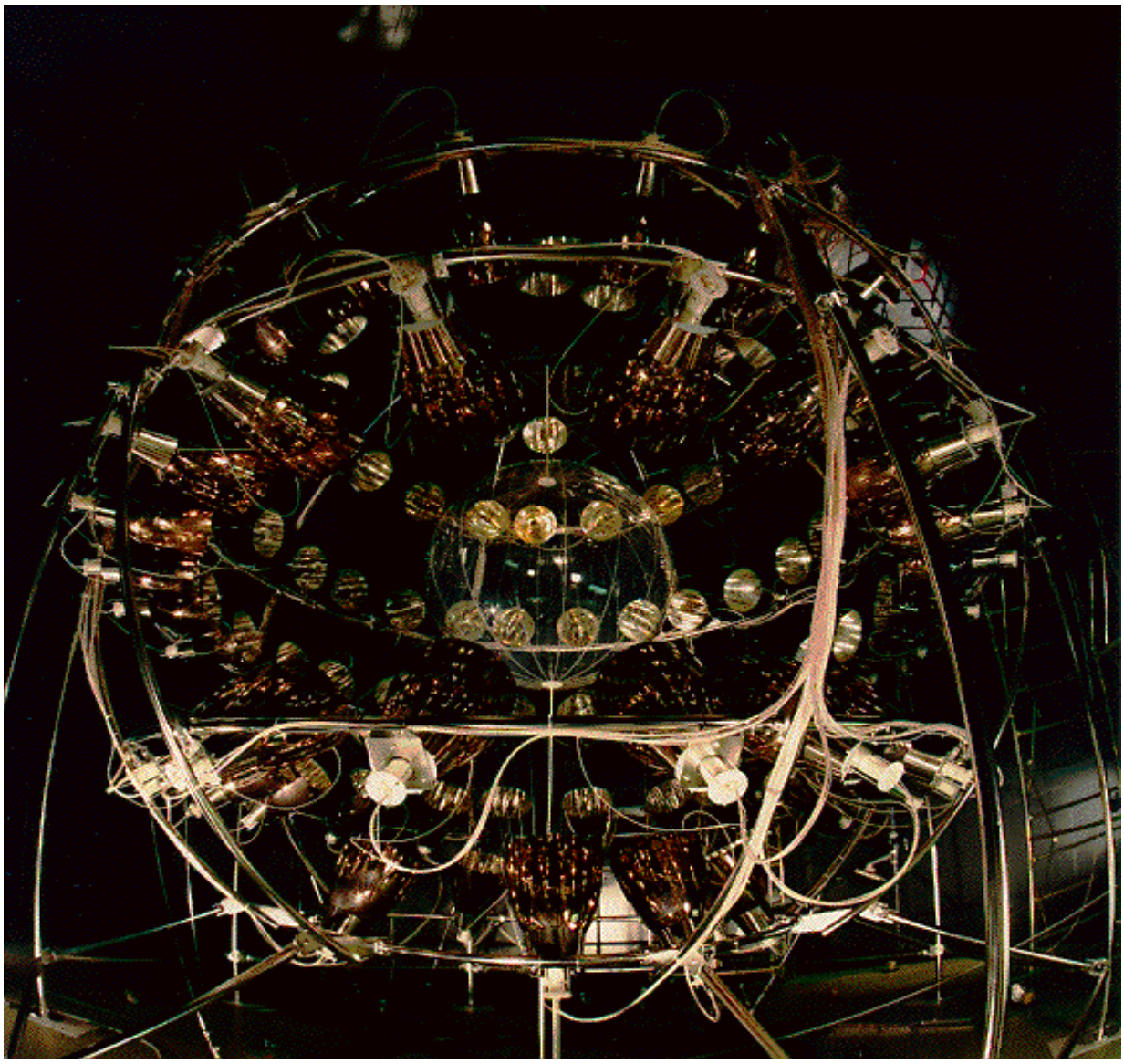

Figure 1: The view of the CTF detector

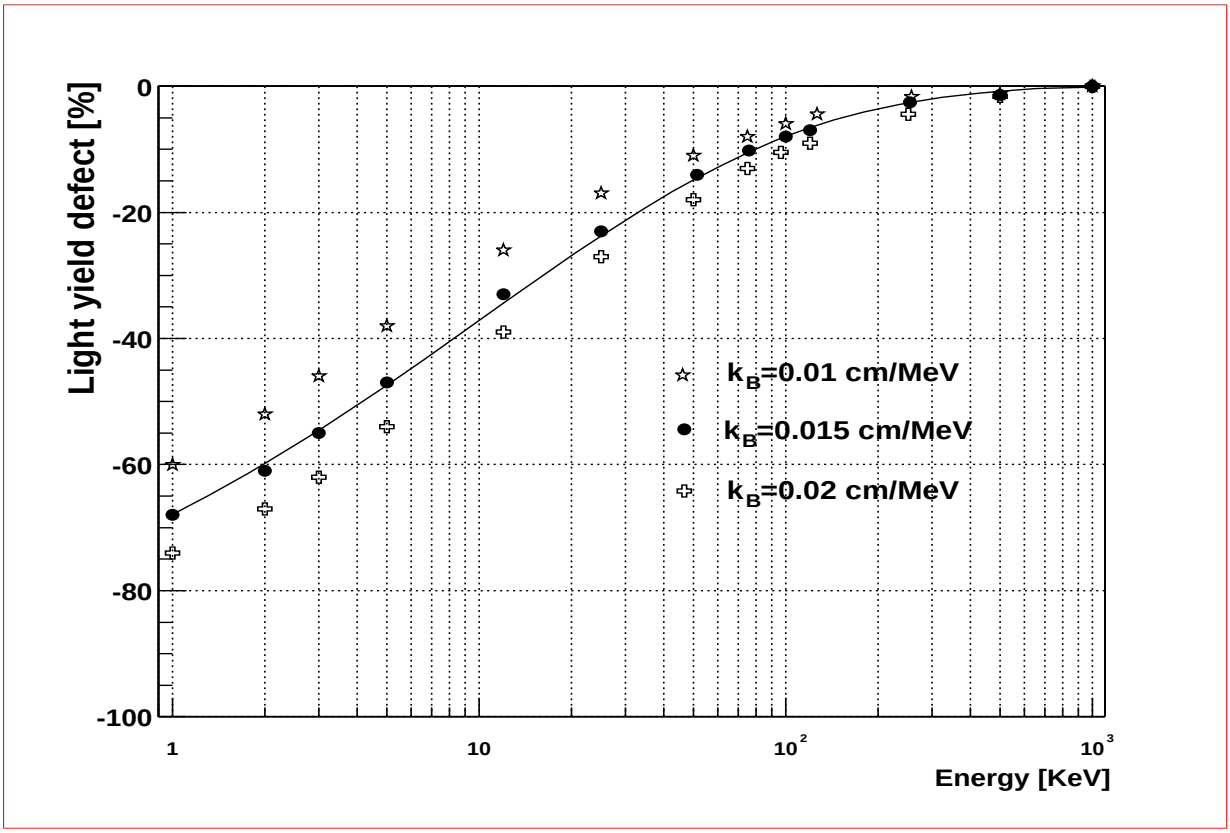

Figure 2: Light yield deficit for 3 different k_B values calculated for PC˙The data for k_B = 0.015 cm/MeV are shown together with fit function (3)

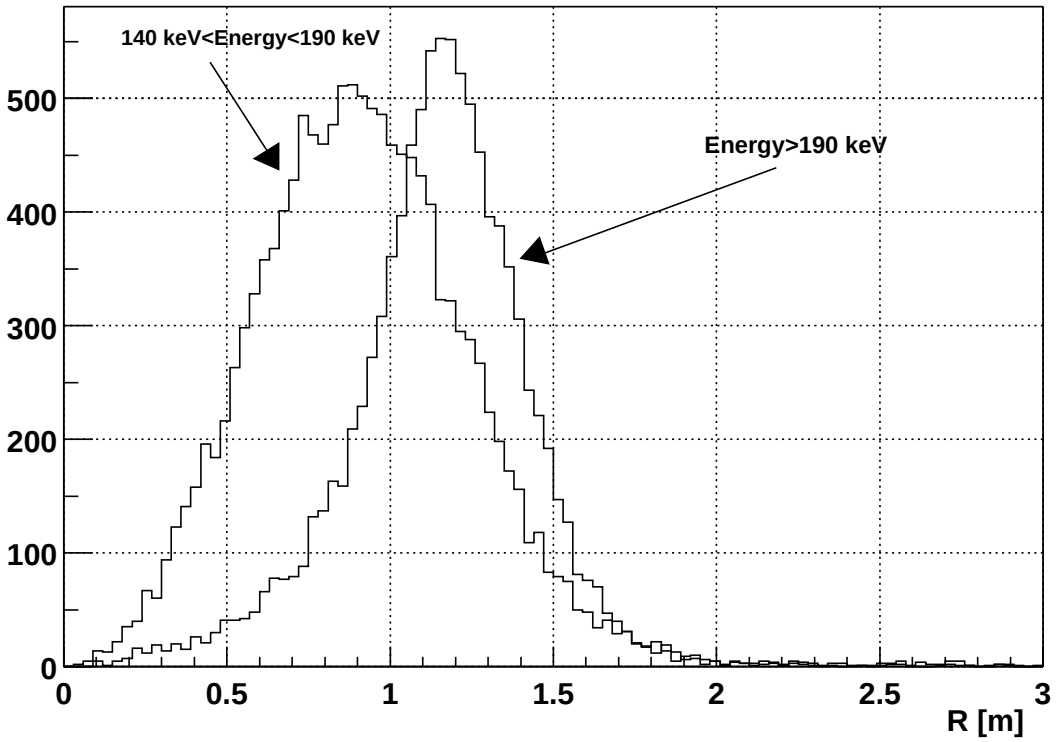

Figure 3: Radial distribution of the events in two different energy intervals. The events in the 140-190 keV interval are mainly ^{14}C events uniformly distributed over the detector's volume with the admixture of the external gammas. The major part of the events with energies greater than 190 keV are the caused by the decay of the ^{40}K, located mainly near the detectors surface.

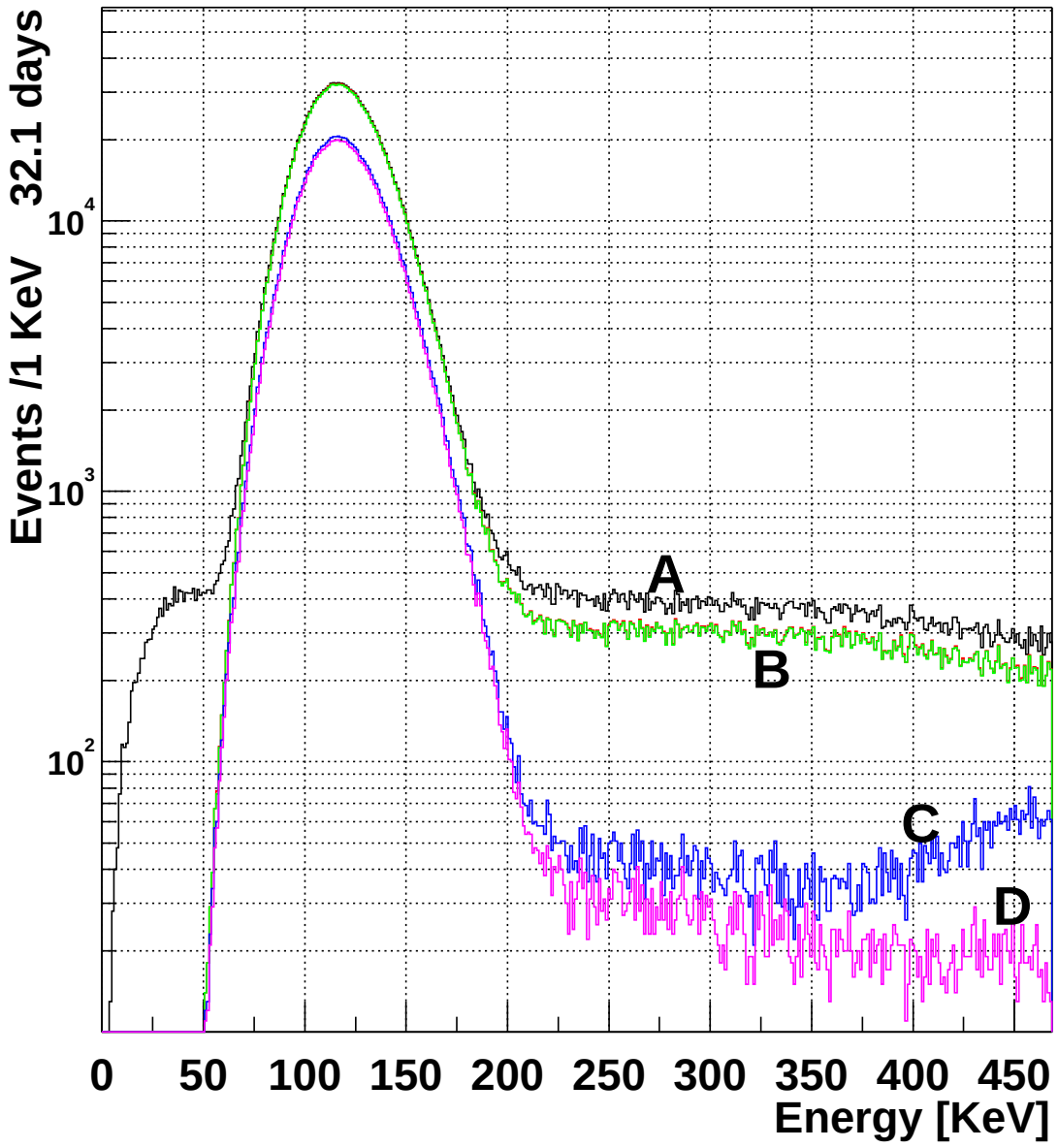

Figure 4: CTF-II background in the low energy region and the result of the sequential cuts applied in order to reduce background: A) raw data; B) muons cut; C) radial cut (with 100 cm radius); D)α/β discrimination.

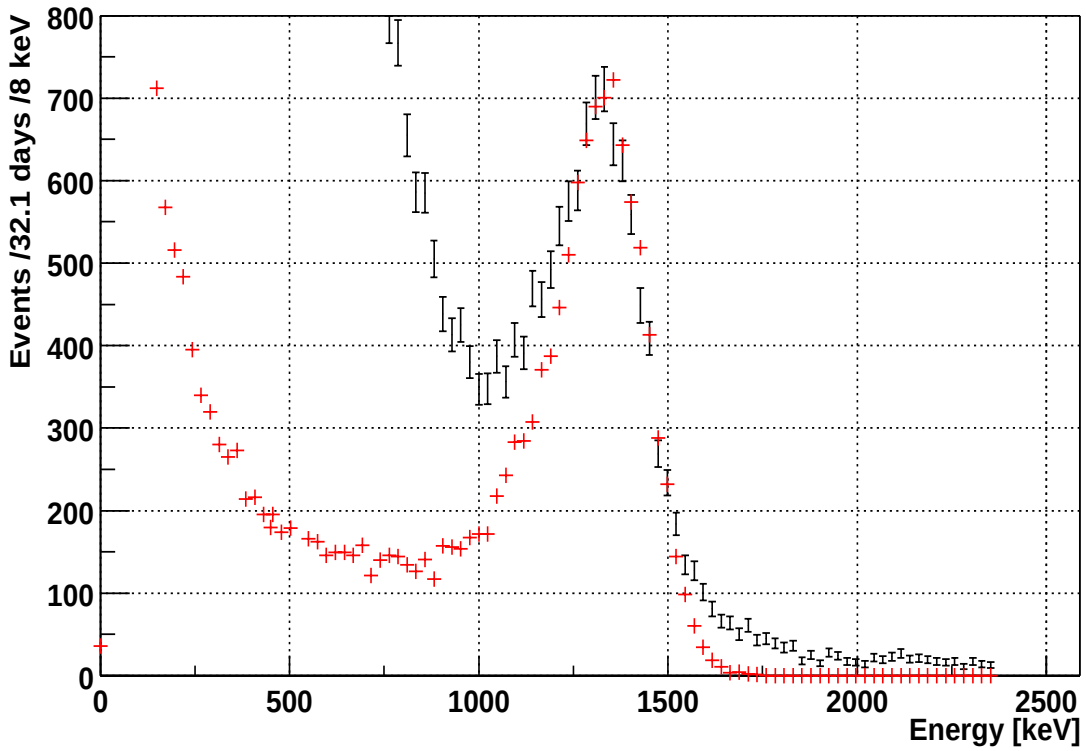

Figure 5: ^{40}K events in the CTF-II data (upper line) and MC simulation of the 1.46 MeV gamma (the lower one). The β-spectrum of the ^{40}K spectrum was not simulated. One can see the good agreement of the position of the peaks

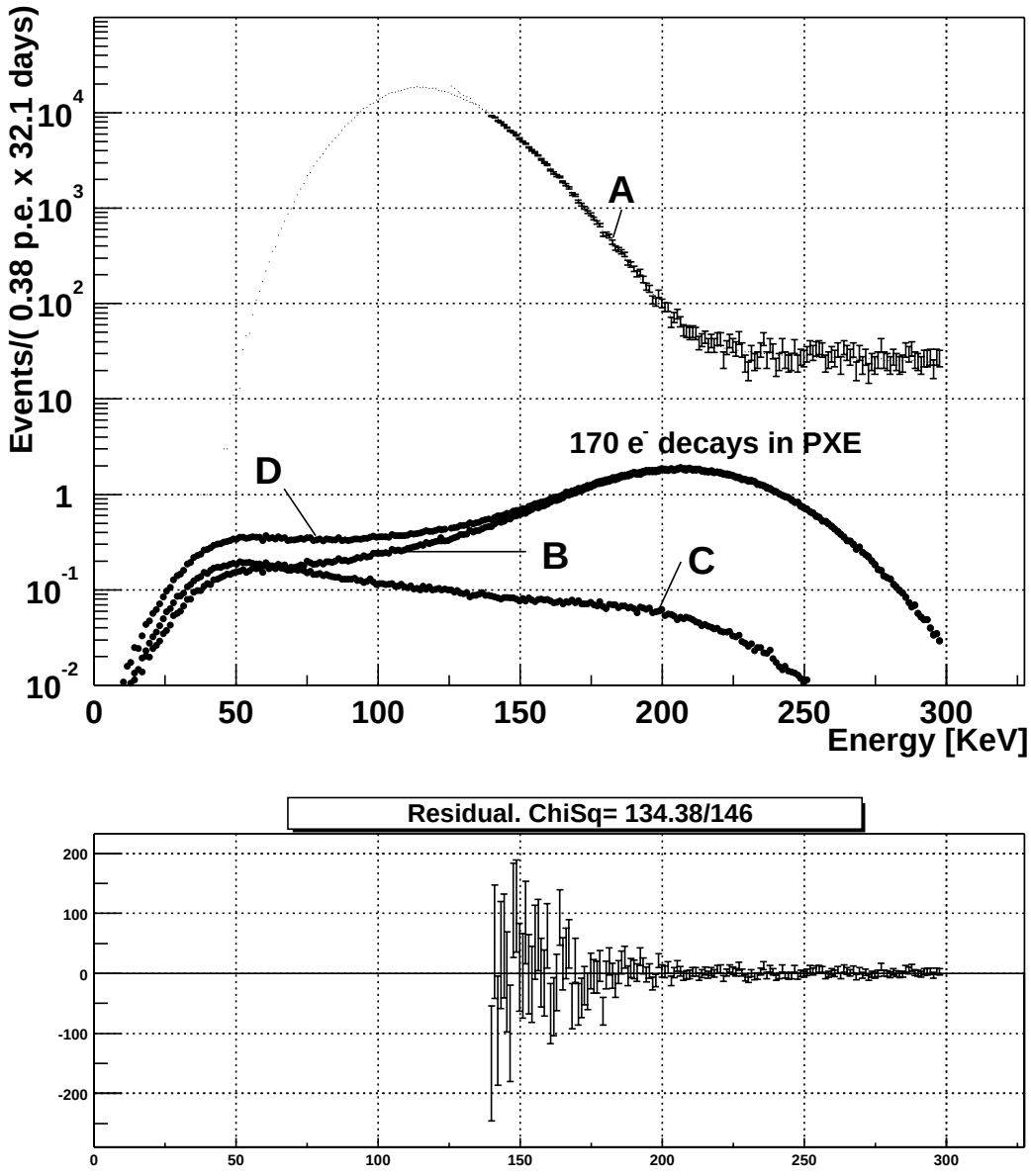

Figure 6: C^{14} spectrum (curve A) with superimposed fit curve and the results of 256 keV γ Monte-Carlo simulations. The Monte-Carlo results are normalized to 170 electron decay events in the inner vessel. An additional gammas, arriving from the decays in surrounding water are shown as well (curve C). The total detector's response to the 256 keV γ (curve D) is the sum of the gammas from PXE (curve B) and water surrounding the inner vessel with PXE (curve C). 0.38 p.e. bin correspond to 1.07 keV at the high energies.